Enfoque UTE, V.9-N.4, Dec.2018, pp. 120 - 130
http://ingenieria.ute.edu.ec/enfoqueute/
e-ISSN: 1390-6542 / p-ISSN: 1390-9363

Recibido (Received): 2018/05/15
Aceptado (Accepted): 2018/11/13

The extended Kalman filter in the dynamic state estimation of electrical power systems

(El filtro extendido de Kalman en la estimación del estado dinámico de sistemas eléctricos de potencia)

Holger Cevallos[1], Gabriel Intriago[1], Douglas Plaza[1], Roger Idrovo[1]

Abstract:
The state estimation and the analysis of load flow are very important subjects in the analysis and management of Electrical Power Systems (EPS). This article describes the state estimation in EPS using the Extended Kalman Filter (EKF) and the method of Holt to linearize the process model and then calculates a performance error index as indicators of its accuracy. Besides, this error index can be used as a reference for further comparison between methodologies for state estimation in EPS such as the Unscented Kalman Filter, the Ensemble Kalman Filter, Monte Carlo methods, and others. Results of error indices obtained in the simulation process agree with the order of magnitude expected and the behavior of the filter is appropriate due to follows adequately the true value of the state variables. The simulation was done using Matlab and the electrical system used corresponds to the IEEE 14 and 30 bus test case systems. State Variables to consider in this study are the voltage and angle magnitudes.

Keywords: state estimation; electric power systems; extended Kalman filter; linear exponential smoothing of Holt; performance indices; IEEE 14 bus test case; IEEE 30 bus test case.

Resumen:
La estimación de estado y el análisis de flujo de carga son tópicos muy importantes en el análisis y control de un Sistema Eléctrico de Potencia (SEP). Este artículo describe la estimación de estados usando el Filtro Extendido de Kalman (EKF) y el método de Holt para linealizar el modelo del proceso y entonces calcular el índice de error del rendimiento del filtro como un indicador de su exactitud. Además, este índice de error calculado puede ser usado como una referencia en posteriores estudios de comparación entre diferentes metodologías usadas en la estimación de estados en SEP tales como el *Unscented* Filtro de Kalman, el *Ensemble* Filtro de Kalman, métodos de Montecarlo, y otros. Los resultados del índice de error obtenidos en el proceso de simulación están de acuerdo al orden de magnitud esperado y el comportamiento del filtro es adecuado ya que sigue adecuadamente al valor verdadero de las variables de estado. La simulación fue realizada usando Matlab y el sistema eléctrico usado corresponde a los sistemas de prueba IEEE de 14 y 30 barras. Las variables de estado a considerar en este estudio son la magnitud del voltaje.

Palabras clave: estimación de estados; sistemas eléctricos de potencia; filtro extendido de Kalman; alisado exponencial lineal de Holt; índices de performance; caso de prueba IEEE de 14 barras; caso de prueba IEEE de 30 barras.

[1] Escuela Superior Politécnica del Litoral, Guayaquil, Ecuador (hcevallos@fiec.espol.edu.ec, gintriag@espol.edu.ec, douplaza@fiec.espol.edu.ec, romiidro@fiec.espol.edu.ec).

1. Introduction

State estimation is an important topic which contributes to the proper management of electrical energy. In this sense, fields where the application of state estimation methods is crucial such as modeling, optimizing power flow, bad data detection, contingencies analysis and corrective actions against possible failures in the power systems improve the monitoring capability of the grid to take control actions in real-time raising the system reliability and stability, (Huang et al., 2012). State estimation is mainly used in the tracking of the dynamics of the power system through the assimilation of real-world information obtained from smart measurement devices.

The Static State Estimation provides the system operating point in a determined time reflected through the state variables for each measurement data set and has no memory of the evolution of the state variables, it was introduced by Schweppe and Wildes (1970), based on Weighted Least Square (WLS). Dynamic State Estimation (DSE) was also introduced by Debs and Larson (1970) with a simple model for the time behavior of the power system.

Kalman filters are widely used for the analysis of dynamic systems with normally distributed noise: the EKF applied for non-linear systems, the unscented Kalman filter, and the ensemble Kalman filter; researchers are also studying the particle filter and other stochastic methods.

In this work, the performance of the EKF focused on forecasting and filtering the state vectors by using exponential smoothing and recursive Bayesian estimation in the state estimation process of the EPS (see *Figures 1 and 2*) can predict state vectors one-time step ahead based on the priori knowledge (prediction stage) and be corrected (update stage) with next measurement sets. The dynamics of the system is simulated using smooth load changes. The loads were changed in each time step with a linear tendency, and the method of Holt has been used to linearize the state transition.

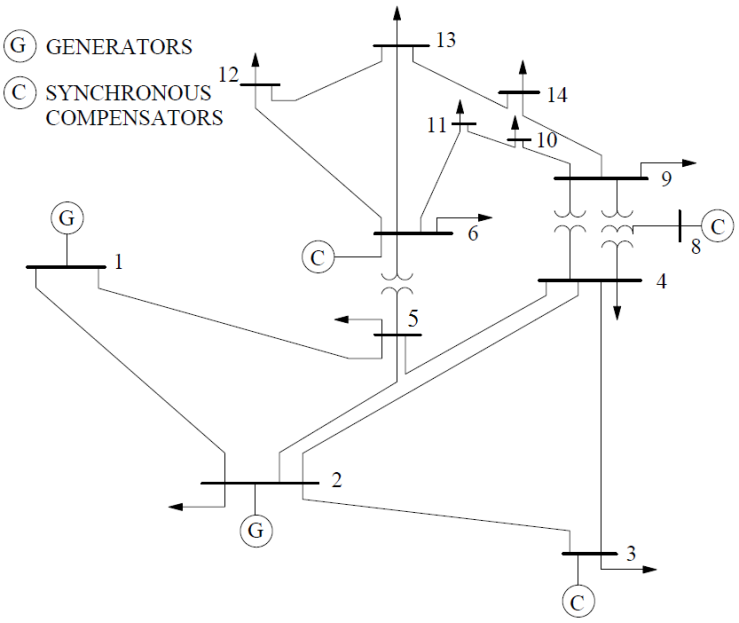

Figure 1. IEEE 14-bus system test case

The electrical power systems with their data considered in the study are the IEEE 14 and 30 bus test cases, which represent a portion of the American Electric Power System (in the Midwestern US) as of February 1962. These and others IEEE n-bus test cases are used as a reference for different studies, and they are found in the archives of the University of Washington (Washington, 1993).

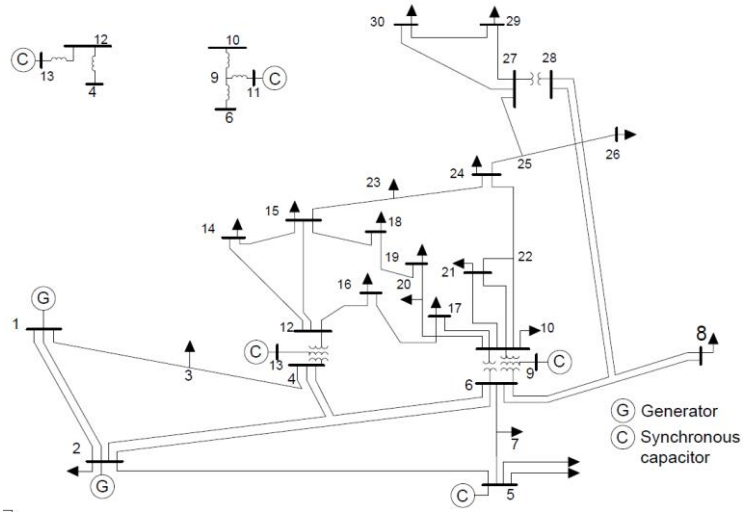

Figura 2. IEEE 30-bus system test case

The extended Kalman filter consists of the linearization of the nonlinear system about a nominal state trajectory and the posterior approximation of the probability density function (pdf) as Gaussian.

The nonlinear system in *Equations 1 and 2* is considered in the derivation of the EKF by using the Recursive Bayesian Estimation approach,

$$x_t = f_{t,t-1}(x_{t-1}) + w_t \quad (1)$$

$$y_t = h_t(x_t) + v_t \quad (2)$$

with $f_{t,t-1}(\cdot)$ the non-linear function relating the state propagation through time and $h_t(\cdot)$ the non-linear observation function. The distributions and statistics of the process and observation noises are presented as shown in *Equations 3 – 8*.

$$w_t \sim \mathcal{N}(w_t: 0, Q_t) \quad (3)$$

$$v_t \sim \mathcal{N}(v_t: 0, R_t) \quad (4)$$

$$E[w_t] = 0\,, E[v_t] = 0, \quad (5)$$

$$E\left[w_t w_{t+k}^T\right] = 0\,, E[w_t w_t^T] = Q_t, \quad (6)$$

$$E\left[v_t v_{t+k}^T\right] = 0\,, E[v_t v_t^T] = R_t, \quad (7)$$

$$E\left[w_t v_{t+k}^T\right] = 0\,, E[w_t v_t^T] = 0, \quad (8)$$

The noises are white Gaussian distributed with zero mean and uncorrelated $\forall t$ with $k \geq 0$, Q and R are positive definite covariances matrices for the process and observation noises respectively, and k is a positive integer.

Based on the fact that the nonlinear system is linearized before the analysis step, the posterior pdf at time step $t-1$ can be approximated by the Gaussian distribution in *Equation 9*,

$$p(x_{t-1}|y_{1:t-1}) \sim \mathcal{N}(x_{t-1}: x_{t-1}^a, P_{t-1}^a) \quad (9)$$

where x_{t-1} is the true state vector, x_{t-1}^a and P_{t-1}^a are the state vector and the covariance matrix, obtained both from the analysis step at time step $t-1$.

Forecast step. The forecast step is given by the computation of the predictive pdf in Equation 10.

$$p(x_t|y_{1:t-1}) = \int p(x_t|x_{t-1})p(x_{t-1}|y_{1:t-1})dx_{t-1} \quad (10)$$

The posterior pdf at time $t-1$ is referred in *Equation 9*. The transition pdf at the right hand side of *Equation 10* can be obtained from *Equation 1* and by considering that this pdf follows the Gaussian distribution in *Equation 11*;

$$p(x_t|x_{t-1}) = \mathcal{N}\big(x_{t-1}: E\big[f_{t,t-1}(x_{t-1})\big], Q_t\big), \quad (11)$$

thus, the predictive pdf is defined as in Equation 12.

$$p(x_t|y_{1:t-1}) = \int \mathcal{N}\big(x_{t-1}: x_{t-1}^a, P_{t-1}^a\big).\mathcal{N}\big(x_{t-1}: E\big[f_{t,t-1}(x_{t-1})\big], Q_t\big)dx_{t-1}, \quad (12)$$

The integral in *Equation 12* is complicated due to the presence of the nonlinear function $f_{t,t-1}(\cdot)$.

The approach adopted in the extended Kalman Filter is the linearization by using Taylor series. Additionally, a state trajectory should be defined around which the function is linearized. At this point in the development of the extended Kalman Filter, the best estimate is given by x_{t-1}^a.

Taylor series expansion of $f_{t,t-1}(x_{t-1})$ in a neighborhood of $x_{t-1}^a = E[x_{t-1}|y_{1:t-1}]$ is considered in the linearization of the system. For the linear approximation, only the first two terms are considered.

The resulting prior pdf can be obtained in the Gaussian form as in *Equation 13*.

$$p(x_t|y_{1:t-1}) = \mathcal{N}(x_t: x_t^f, P_t^f), \quad (13)$$

The forecast state vector x_t^f and forecast error covariance matrix P_t^f are given by *Equations 14 and 15*.

$$x_t^f = f_{t,t-1}(x_{t-1}^a) \quad (14)$$

$$P_t^f = F_{t,t-1}P_{t-1}^a F_{t,t-1}^T + Q_t \quad (15)$$

Analysis step. The analysis step consists in the update of the prior according to *Equation 16*.

$$p(x_t|y_{1:t}) = \frac{p(y_t|x_t)p(x_t|y_{1:t-1})}{\int p(y_t|x_t)\, p(x_t)|y_{1:t-1}dx_t} \quad (16)$$

For the extended Kalman filter, the prior is approximated by a Gaussian distribution which is characterized by the mean (*Equation 14*) and the covariance (*Equation 15*). The likelihood pdf is obtained from Equation 2, by considering that the pdf in *Equation 17* is Gaussian.

$$p(y_t|x_t) = \mathcal{N}(y_t: E[h_t(x_t)], R_t) \quad (17)$$

By substituting *Equation 13* and *Equation 17* into *Equation 16*, the filtering pdf is given by *Equation 18*,

$$p(x_t|y_{1:t}) = \frac{\mathcal{N}(y_t: E[h_t(x_t)], R_t)\mathcal{N}(x_t: x_t^f: P_t^f)}{\int \mathcal{N}(y_t: E[h_t(x_t)], R_t)\mathcal{N}(x_t: x_t^f: P_t^f)dx_t} \quad (18)$$

where the first issue aiming to calculate the filtering pdf is to solve the integral in the denominator. In order to find an analytical solution, the observation system is linearized around a state trajectory. At this point, x_t^f is the best state estimation thus the nonlinear observation system is linearized through Taylor series expansion in the neighborhood of x_t^f. The non-linear function is expanded as in *Equation 19*,

$$h_t(x_t) \simeq h_t\left(x_t^f\right) + H_t[x_t - x_t^f] \tag{19}$$

where H_t is a $(m_y \times m_x)$ dimensional Jacobian matrix.

By substituting *Equation 19* into *Equation 18*, the expression for the posterior pdf is given in *Equation 20*.

$$p(x_t|y_{1:t}) = \frac{\mathcal{N}(y_t: h_t\left(x_t^f\right) + H_t\left[x_t - x_t^f\right], R_t)\mathcal{N}(x_t: x_t^f: P_t^f)}{\int \mathcal{N}(y_t: h_t\left(x_t^f\right) + H_t\left[x_t - x_t^f\right], R_t)\mathcal{N}(x_t: x_t^f: P_t^f)dx_t} \tag{20}$$

Now, the solution of the integral is tractable, and the resulting expression for the posterior pdf in terms of distribution is (Equation 21):

$$p(x_t|y_{1:t}) = \mathcal{N}(x_t^a, P_t^a); \tag{21}$$

with (*Equations 22 and 23*)

$$x_t^a = x_t^f + K_t\left(y_t - h_t\left(x_t^f\right)\right), \tag{22}$$

$$P_t^a = P_t^f - K_t H_t P_t^f, \tag{23}$$

and *Equation 24*.

$$K_t = P_t^f H_t^T [H_t P_t^f H_t^T + R_t]^{-1} \tag{24}$$

The algorithm for the extended Kalman filter is described in *Algorithm 1*.

Algorithm 1. Extended Kalman Filter
For $t = 1$ to the number of time steps
1. Forecast step:
   $x_t^f = f_{t,t-1}(x_{t-1}^a)$
   $P_t^f = F_{t,t-1}P_{t-1}^a F_{t,t-1}^T + Q_t$
2. Analysis step:
   $K_t = P_t^f H_t^T [H_t P_t^f H_t^T + R_t]^{-1}$
   $x_t^a = x_t^f + K_t(y_t - h_t(x_t^f))$
   $P_t^a = P_t^f - K_t H_t P_t^f$

2. Methodology

The Electrical Power System

To simulate the slow dynamics of the test systems under normal conditions, the smooth load changes were obtained by running load flow calculations under different loading conditions at each step (Valverde and Terzija, 2011). The dynamics of the system was obtained by varying the loads at certain predefined buses (4, 5, 7, 9-14 for the 14- bus system and 3, 4, 6, 7, 9, 10, 12, 14-30 for the 30- bus system) following a linear trend of 1% over the entire time interval with a random fluctuation of 3%. Additionally, measurements of voltage, power injections, and power transfer were corrupted with a random additive

Gaussian distributed noise with a mean equal to zero and a low level of variability, this is, with a standard deviation (σ) according to *Table 1* (Sharma, Srivastava, and Chakrabarti, 2017) for voltage and powers respectively, to consider the uncertainty of measurement.

Table 1. Values of standard deviation Measurement $\sqrt{R_k}$

Power Injection in pu.	0.001
Power Flow in pu.	0.001
Voltage in pu.	0.0006
Angle in rad.	0.018

The state variables were the voltage (v) and angle (θ) magnitudes of each one of the bars. Bus 1, in both systems, was considered the slack bus with angle 0°. Buses 1, 2, 3, 6, 9 for the 14-bus system and buses 1, 2, 5, 8, 11, 13 for the 30-bus system were buses with a regulated voltage. The 14-bus system had 73 measurements, from which 5 were voltage magnitudes, and the rest were power magnitudes. The 30-bus system had 93 measurements, from which all were power magnitudes except the first that was a voltage magnitude.

Performance indices

The accuracy of EKF are carried out using the following indices as seen in previous studies (Alhalali and Elshatshat, 2015; Valverde and Terzija, 2011):

(1) The error estimation $\varepsilon(\mathrm{k})$ for step k (*Equation 25*):

$$\varepsilon(k) = \frac{1}{2N_{barras} - 1} * \sum_{n=2}^{2N_{barras}} |\hat{x}_n(k) - x_n^t(k)| \tag{25}$$

(2) The error estimation $\varepsilon(\mathrm{n})$ for bus n:

- $\varepsilon_v(n)$ for voltage magnitude (*Equation 26*):

$$\varepsilon_v(n) = \frac{1}{N_{pasos}} * \sum_{k=1}^{N_{pasos}} \left|\hat{v}_k(n) - v_k^t(n)\right| \tag{26}$$

- $\varepsilon_\theta(n)$ for angle magnitude (*Equation 27*):

$$\varepsilon_\theta(n) = \frac{1}{N_{pasos}} * \sum_{k=1}^{N_{pasos}} \left|\hat{\theta}_k(n) - \theta_k^t(n)\right| \tag{27}$$

(3) The performance index $J(k)$ (*Equation 28*):

$$J(k) = \frac{\sum_{i=1}^{m}\left|\hat{z}_i(k) - z_i^t(k)\right|}{\sum_{i=1}^{m}\left|z_i(k) - z_i^t(k)\right|} \tag{28}$$

where, x is the state vector$[\theta_2 \dots \theta_n v_1 \dots v_n]$, $\varepsilon(k)$ is the mean error for the k^{th}, $\hat{x}_n(k)$ is the filtered (estimated) state vector at k^{th} step and n^{th} bus, N_{buses} is the number of buses, $\varepsilon(n)$ is the mean error for the n^{th} bus, $\varepsilon_v(n)$ is the error estimation calculated for voltage magnitude at n^{th} bus, $\hat{v}_k(n)$ is the filtered (estimated) voltage magnitude at n^{th} bus and k^{th} step, $v_k^t(n)$ is the true (actual) voltage magnitude at n^{th} bus and k^{th} step, $\varepsilon_\theta(n)$ is

the error estimation calculated for angle magnitude at n^{th} bus, $\hat{\theta}_k(n)$ is the filtered (estimated) angle magnitude at n^{th} and k^{th} step, $\theta_k^t(n)$ is the true (actual) angle magnitude at n^{th} and k^{th} step, N_{steps} is the number of time steps (sampling time), $J(k)$ is the calculated performance index for step k, m is the number of measurements (observations), $\hat{z}_i(k)$ is the estimated measurement vector at i^{th} measurement and k^{th} step, $z_i(k)$ the real measurement vector at i^{th} measurement and k^{th} step, $z_i^t(k)$ is the true measurement vector at i^{th} measurement and k^{th} step.

Extended Kalman Filter – EKF

The non-linear stochastic difference equations that govern the system with a state vector $x \in \Re^n$ is (*Equation 29*):

$$x_k = f(x_{k-1}, u_k, w_{k-1}) \tag{29}$$

with a measurement vector $z \in \Re^m$, that is (*Equation 30*):

$$z_k = h(x_k, v_k) \tag{30}$$

where u_k represents any driving function , the random variables w_k and v_k represent the process and measurement noise and assumed to be independent (of each other), white, and with normal probability distribution: $p(w) \sim N(0, Q_{k-1}), p(v) \sim N(0, R_k)$ respectively.

The Gaussian process noise error covariance (Q_{k-1}) and the measurement noise error covariance R_k are diagonal matrices that might change with each time step or measurement (Zanni, Le Boudec, Cherkaoui, and Paolone, 2017). In this study, the Q_{k-1} value was kept constant and set to 10^{-6} according to Valverde and Terzija (2011). The values for the standard deviation of measurement noise error variance $\sqrt{\mathrm{R_k}}$, were taken from the *Table 1* as used in Sharma et al. (2017).

As the most used approach to handle the complexity of model mentioned above, the EKF-based method is to linearize (29), assuming a quasi-steady-state behavior of the system, it can be represented by *Equation 31*,

$$x_k = F_{k-1} * x_{k-1} + g_{k-1} + q_{k-1} \tag{31}$$

where matrix F_{k-1} represents the transition speed between states; vector g_{k-1} is related with the behavior tendency of the states. Dynamic State Estimation depends strongly on the forecasting technique chosen to estimate parametersF_{k-1}, g_{k-1} and q_{k-1}. The technique used in this document for calculating F_{k-1} and g_{k-1} Linear exponential smoothing of Holt (online parameter identification technique) widely used to forecast the states in this type of work (Leite da Silva, Do Coutto Filho, and De Queiroz, 1983; Nguyen, Venayagamoorthy, Kling, and Ribeiro, 2013; Valverde and Terzija, 2011) which provides good predictions even when state variables are assumed to be independent. Values of these parameters can be obtained as in *Equations 32 and 33*,

$$F_{k-1} = \alpha_{k-1}(1 + \beta_{k-1})I, \tag{32}$$

$$g_{k-1} = (1 + \beta_{k-1})(1 - \alpha_{k-1})\tilde{x}_{k-1} - \beta_{k-1}a_{k-2} + (1 - \beta_{k-1})\, b_{k-2} \tag{33}$$

where $\tilde{x}_{k-1}$ is the predicted state vector at step $k-1$, I is the identity matrix, the parametersα_{k-1} and β_{k-1} are between 0 and 1 in this work have been fixed constant throughout the whole simulation to 0.5 and 0.8 respectively as proposed in Valverde and Terzija (2011), and the vectors a and b can be obtained from previous (a priori) knowledge (*Equations 34 and 35*),

$$a_{k-1} = \alpha_{k-1} x_{k-1}^{t} + (1 - \alpha_{k-1})\tilde{x}_{k-1}, \quad (34)$$

$$b_{k-1} = \beta_{k-1}(a_{k-1} - a_{k-2}) + (1 - \beta_{k-1})\, b_{k-2} \quad (35)$$

where $\tilde{x}_{k-1}$ is the predicted state vector and, x_{k-1}^{t} is the true state vector.

Active and reactive power balance, line flow equations and bus voltages govern the non-linear function $h(\cdot)$ that relates measurement z_k with the state vectors. The flowchart for the EKF method is illustrated in *Figure 3*.

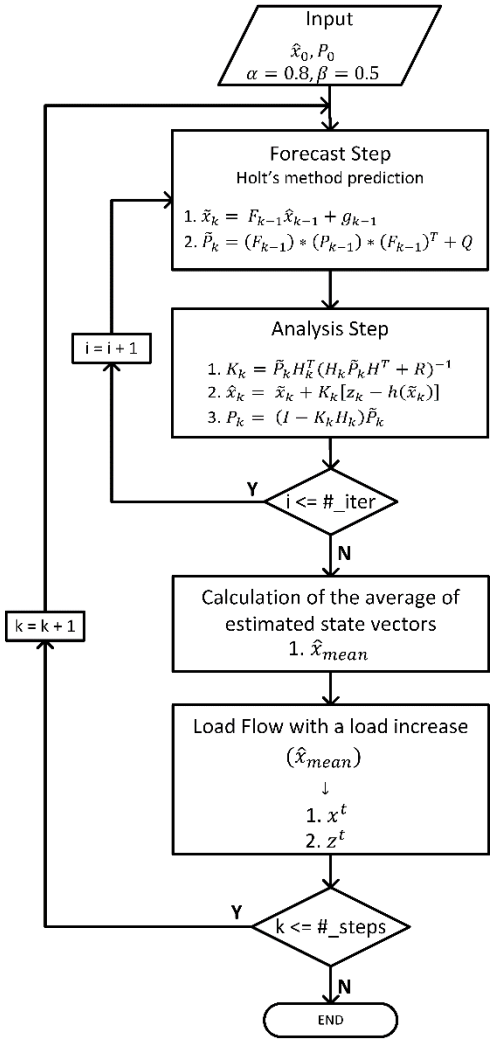

Figure 3. Flow Chart of EKF Algorithm.

3. Results and discussion

The proposed calculation of the error (ε) and performance ($\mathcal{J}$) indices, and their respective standard deviation are presented in *Table 2* for 14 and 30 buses

Table 2. Index error for EKF and standard deviations (σ) for 14 and 30 buses

Buses	Index	EKF	σEKF
14	$\varepsilon_v(n) * 10^{-3}, pu$	0.26995	0.13941
	$\varepsilon_\theta(n) * 10^{-3}, pu$	0.40309	0.17706
	$\varepsilon(k) * 10^{-3}, pu$	0.34899	0.44329
	$J(k)$	0.72139	0.07470
30	$\varepsilon_v(n) * 10^{-3}, pu$	1.4533	0.48266
	$\varepsilon_\theta(n) * 10^{-3}, pu$	1.9930	0.75792
	$\varepsilon(k) * 10^{-3}, pu$	1.7524	0.75503
	$J(k)$	0.84601	0.06132

Table 2 shows that the average of the ($\mathcal{J}$) index and the average errors of the 30-bus system are higher than the equivalent averages of the 14-bus system.

The *Figures 4 to 8* show the evolution of error indices (ε) and performance indices ($\mathcal{J}$) according to definitions established before for 14 and 30 bus systems

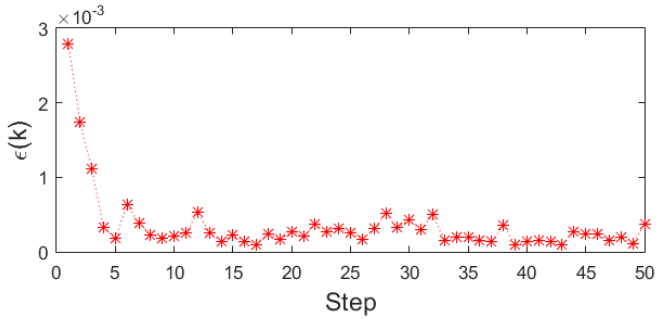

Figure 4. Estimation error for step k - 14 bus test case.

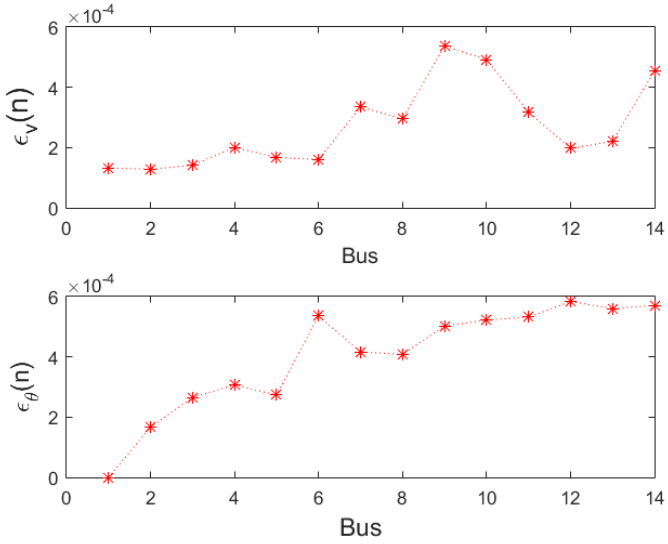

Figure 5. Voltage and angle magnitude error for bus n - 14 bus test case.

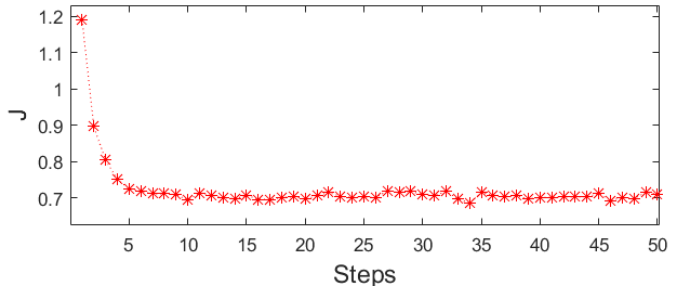

Figure 6. J performance index - 14 bus test case.

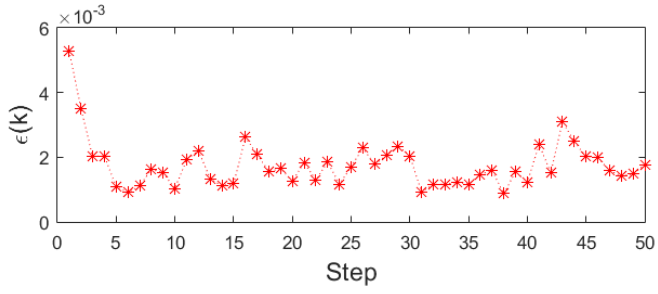

Figure 7. Estimation error for step k - 30 bus test case.

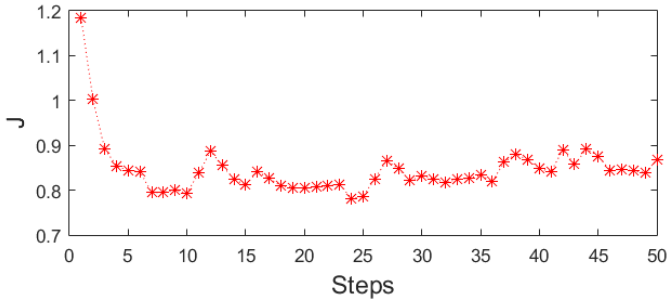

Figure 8. J performance index - 30 bus test case.

Figure 5 shows the voltage and angle magnitude error for each bus during the 50 steps of our simulation. *Figure 4* and *Figure 7* present the estimation error of each simulation step considering the 2n−1 state variables of each system. The performance index ($\mathcal{J}$), in *Figure 6* has a peak in the first steps because of the difference between the initial estimated values and the true values of the measurements is high.

The *Figures 9 to 12* show the behavior of the estimation values concerning the true values of voltage and angle magnitudes. It can be seen that in all the graphs there is a tracking of the estimation signal towards the real signal.

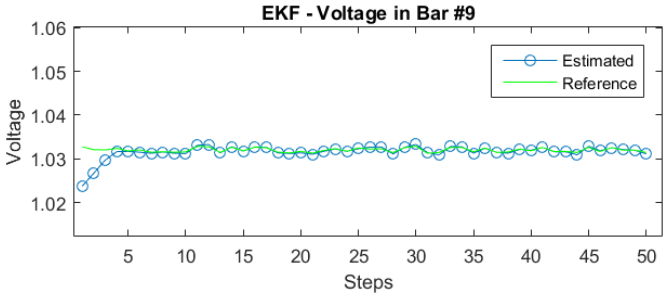

Figure 9. Voltage magnitude in bar 9 - 14 bus test case.

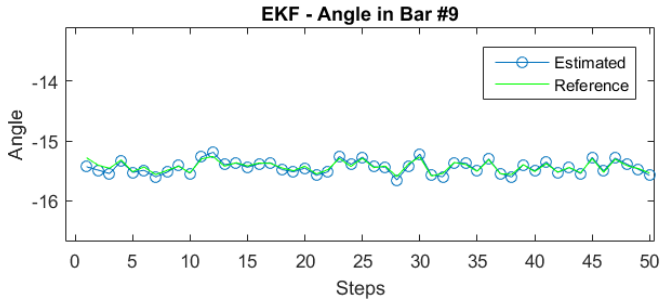

Figure 10. Angle magnitude in bar 9 - 14 bus test case.

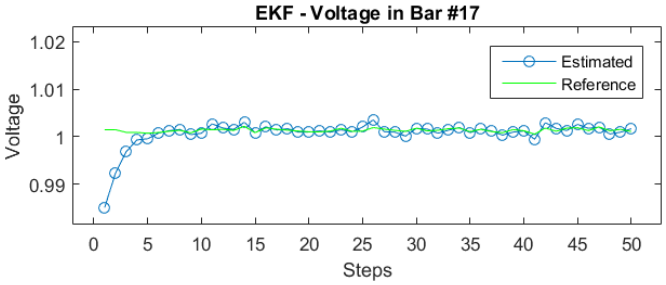

Figure 11. Voltage magnitude in bar 17 - 30 bus test case.

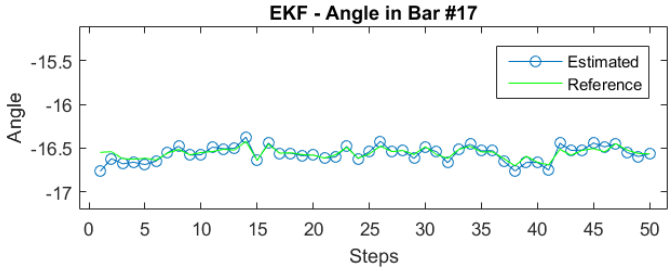

Figure 12. Angle magnitude in bar 17 - 30 bus test case.

4. Conclusion and recommendations

In general, it can be concluded that the methodology used in this work to estimate states of an EPS is showing good results and the error indices reported can be accepted as referential values in this types of studies, e.g., to compare accuracies between different methods employed to state estimation of EPS. Future work will study the Monte Carlo methods deeply in the state estimation of EPS such as the Ensemble Kalman Filter and sequential Monte Carlo methods.

References

Alhalali, S.M.O., and Elshatshat, R.A. (2015). "State Estimator for Electrical Distribution Systems Based on a Particle Filter". *2015 IEEE Power & Energy Society General Meeting,* p. 1-5. http://dx.doi.org/10.1109/PESGM.2015.7286398

Debs, A.S., and Larson, R.E. (1970). "A Dynamic Estimator for Tracking the State of a Power System". IEEE Transactions on Power Apparatus and Systems, PAS-89(7), p. 1670-1678. http://dx.doi.org/10.1109/TPAS.1970.292822

Huang, Y.F., Werner, S., Huang J., Kashyap N., and Gupta V. (2012). "State Estimation in Electric Power Grids: Meeting New Challenges Presented by the Requirements of the Future Grid". *IEEE Signal Processing Magazine*, 29(5), p. 33-43. http://dx.doi.org/10.1109/MSP.2012.2187037

Leite da Silva, A.M., Do Coutto Filho, M.B., and De Queiroz, J.F. (1983). "State forecasting in electric power systems". *IEEE Proceedings C – Generation, Transmission and Distribution,* 130(5), p. 237-244. http://dx.doi.org/10.1049/ip-c:19830046

Nguyen, H., Venayagamoorthy, G., Kling, W. and Ribeiro, P. (2013). Dynamic state estimation and prediction for real-time control and operation. *Power Systems Conference (PS13)*. Technische Universiteit Eindhoven.

Schweppe, F., and Wildes, J. (1970). "Power System Static-State Estimation, Part I: Exact Model". *IEEE Transactions on Power Apparatus and Systems,* PAS-89(1), p. 120-125. http://dx.doi.org/10.1109/TPAS.1970.292678. Recuperado de htttp://ieeexplore.ieee.org/lpdocs/epic03/wrapper.htm?arnumber=4074022 (accedido el 20/02/2018).

Sharma, A., Srivastava, S.C., and Chakrabarti, S. (2017). "A Cubature Kalman Filter Based Power System Dynamic State Estimator". *IEEE Transactions on Instrumentation and Measurement,* 66(8), p. 2036-2045. http://dx.doi.org/10.1109/TIM.2017.2677698

University of Washington. (1993). "IEEE 14 bus test case". Recuperado de http://www2.ee.washington.edu/research/pstca/pf14/ieee14cdf.txt (accedido el 20/03/2018).

Valverde, G., and Terzija, V. (2011). "Unscented kalman filter for power system dynamic state estimation". *Generation, Transmission & Distribution IET,* 5(1), p. 29-37.

Zanni. L., Le Boudec, J.Y., Cherkaoui, R., and Paolone, M. (2017). "A Prediction-Error Covariance Estimator for Adaptive Kalman Filtering in Step-Varying Processes: Application to Power-System State Estimation". *IEEE Transactions on Control Systems Technology*, 25(5). http://dx.doi.org/10.1109/TCST.2016.2628716.